

R E M A R K S

The Applicants note that all amendments and cancellations of Claims are made without acquiescing to any of the Examiner's arguments or rejections, and solely for the purpose of expediting the patent application process in a manner consistent with the PTO's Patent Business Goals (PBG),¹ and without waiving the right to prosecute the cancelled claims (or similar claims) in the future.

The Examiner has stated that the previously filed Invention Disclosure Statement of 05/10/2004 failed to comply with 37 CFR 1.98(a)(2) because the IDS does not include a legible copy of the Ford et al., Science 2001; 291:1051 reference (Office Action, pg. 3). The Applicants have attached a new copy of the Ford et al. reference to this communication and respectfully request that the reference be considered.

In the Final Office Action dated 10/31/06, the Examiner issued two rejections. Each of the rejections is discussed below.

I. The Claims are Definite

The Examiner rejects Claims 1 and 3-11 under 35 U.S.C. 112, second paragraph, as allegedly being incomplete for omitting essential steps (Office Action, pg. 3). The allegedly omitted steps are: a reference or control. The Applicants respectfully disagree. Nonetheless, in order to further the business interests of the Applicants and while reserving the right to prosecute the original (or similar) claims in the future, the Applicants have amended Claim 1 to include additional language of an absence of antibodies to HIP1 being indicative of an absence of prostate cancer in the subject. As such, the Applicants believe that the rejection should be withdrawn.

II. The Claims are Enabled

The Examiner rejects Claims 1-11 under 35 U.S.C. 112, first paragraph, as allegedly lacking enablement (Office Action, pg. 4). In particular, the Examiner states "Thus, the claims imply that the presence or absence of antibodies to HIP1 in any sample can be used to detect any/and or all cancers." (Office Action, pg. 4). The Applicants respectfully disagree. The

¹ 65 Fed. Reg. 54603 (Sept., 8, 2000).

claims are clearly directed towards detection of **prostate** cancer: “wherein the presence of antibodies to HIP1 in said sample is indicative of prostate cancer in said subject” (Claim 1). Nonetheless, in order to further the business interests of the Applicants and while reserving the right to prosecute the original (or similar) claims in the future, the Applicants have amended the preamble of Claim 1 to refer to a method for detecting prostate cancer. The Applicants have further amended Claim 1 to specify that the sample is a serum sample. As such, the Applicants submit that the Examiner’s statement that the claims are directed towards detecting any cancer in any sample is moot.

The Examiner further states: “In other words, 25% of the prostate cancer patient cohort was positive for a humoral response to HIP1, whereas 39% of the “normal” patient cohort were positive. In view of this teaching, it appears that the presence of antibodies to HIP, e.g., positive humoral response to HIP1, would be more indicative of a “normal” patient and not of a patient suffering from prostate cancer.” (Office Action, pg. 6). The Applicants respectfully disagree. The Applicants attach hereto a publication by the inventors utilizing a larger cohort of patients that demonstrates, per the teachings of the specification, a correlation between antibodies to HIP1 and prostate cancer (Bradley et al., Cancer Res. 65:4126 [2005]). In particular, Figure 3 (Western blot; pg. 4130) and Figure 4 (ELISA; pg. 4131) demonstrate that a higher percentage of prostate cancer patients relative to control individuals demonstrated a humoral response to HIP1. As such, the Applicants submit that the application is enabled for detection of a correlation between serum antibodies to HIP1 and prostate cancer. Accordingly, the Applicants submit that the claims are enabled and respectfully request that the rejection be withdrawn.

CONCLUSION

If a telephone interview would aid in the prosecution of this application, the Examiner is encouraged to call the undersigned collect at (618) 218-6900.

Dated: January 3, 2007



Tanya A Arenson
Reg. No. 47,391

MEDLEN & CARROLL, LLP
101 Howard Street, Suite 350
San Francisco, California 94105
608.218.6900

REPORTS

hours after transfection. COS-7 cells were incubated with EGF (0.1 μ g/ml) [biotinylated, complexed to Texas Red-streptavidin (Molecular Probes, Eugene, OR)] in binding buffer [20 mM Hepes-NaOH (pH 7.5), 130 mM NaCl, and 0.1% bovine serum albumin] at 4°C for 60 min. Internalization of EGF was allowed by incubation in Dulbecco's modified

Eagle's medium at 37°C for 10 min, then excess EGF was removed with 0.2 M AcOH (pH 2.5) and 0.5 M NaCl at 4°C for 5 min. Cells were fixed in 3.7% formaldehyde, permeabilized with 0.2% Triton X-100, and immunostained with a polyclonal antibody to myc (Santa Cruz Biotechnology, Santa Cruz, CA) and fluorescein isothiocyanate-conju-

gated antibody to rabbit (Organon Teknika, Bostel, Netherlands). Internalization of EGF was observed by confocal microscopy (Bio-Rad).

37. We thank Y. Watanabe (Ehime University, Japan) for providing us with various synthetic phosphoinositides.

16 October 2000; accepted 15 December 2000

Simultaneous Binding of PtdIns(4,5)P₂ and Clathrin by AP180 in the Nucleation of Clathrin Lattices on Membranes

Marijn G. J. Ford, Barbara M. F. Pearse, Matthew K. Higgins, Yvonne Vallis, David J. Owen, Adele Gibson,* Colin R. Hopkins,* Philip R. Evans,† Harvey T. McMahon†

Adaptor protein 180 (AP180) and its homolog, clathrin assembly lymphoid myeloid leukemia protein (CALM), are closely related proteins that play important roles in clathrin-mediated endocytosis. Here, we present the structure of the NH₂-terminal domain of CALM bound to phosphatidylinositol-4,5-bisphosphate [PtdIns(4,5)P₂] via a lysine-rich motif. This motif is found in other proteins predicted to have domains of similar structure (for example, Huntingtin interacting protein 1). The structure is in part similar to the epsin NH₂-terminal (ENTH) domain, but epsin lacks the PtdIns(4,5)P₂-binding site. Because AP180 could bind to PtdIns(4,5)P₂ and clathrin simultaneously, it may serve to tether clathrin to the membrane. This was shown by using purified components and a budding assay on preformed lipid monolayers. In the presence of AP180, clathrin lattices formed on the monolayer. When AP2 was also present, coated pits were formed.

Budding of clathrin-coated vesicles is a process by which cells package specific cargo into vesicles in a regulated fashion (1–3). Important functions are the uptake of nutrients, the regulation of receptor and transporter numbers on the plasma membrane, and the recycling of synaptic vesicles. AP180 and AP2 are both major components of clathrin coats. AP2 is a heterotetrameric complex that binds to phosphoinositides in the membrane and to the cytoplasmic domains of membrane proteins destined for internalization (1, 3, 4). AP2 binds clathrin and can stimulate clathrin cage assembly in vitro (5, 6). It also interacts with a range of cytoplasmic proteins including AP180 (7). Like AP2, AP180 also binds directly to clathrin and can stimulate clathrin cage assembly in vitro, limiting the size distribution of the resulting cages (8–11). The related proteins, CALM (AP180-2, a close homolog of synaptic AP180), LAP (the *Drosophila* AP180 homolog), and UNC-11 (the

Caenorhabditis elegans homolog), are all implicated in clathrin-coated vesicle endocytosis (12, 13). CALM was identified and named because of its homology to AP180 and to reflect its involvement in t(10;11) chromosomal translocations found in various leukemias (14). Disruptions of the *LAP* and *Unc-11* genes impair clathrin-dependent recycling of synaptic vesicles, resulting in fewer vesicles of more variable size. The NH₂-terminal domain of AP180 (AP180-N) shows the highest degree of conservation across AP180 homologs, and binds to inositol polyphosphates (10, 15, 16), whereas the COOH-terminal domain contains the putative clathrin- and AP2-binding sites (Fig. 1A).

When expressed in COS-7 fibroblasts, both full-length AP180 and AP180-C (residues 530 to 915) inhibited uptake of epidermal growth factor (EGF) and transferrin (17) (Fig. 1B), as is the case for CALM (18). Clathrin was redistributed in transfected cells, and we noted fewer coated pits per unit of cell surface-membrane length (8% of control, Fig. 1C). This showed that endocytosis was inhibited by blocking clathrin-coated pit formation, consistent with the ability of the COOH-terminus to bind clathrin and to stimulate cage assembly in vitro (8–11). However, AP180-N overexpression did not inhibit EGF or transferrin uptake (Fig. 1B).

It had no apparent protein-binding partners but is more localized to the plasma membrane, consistent with binding to polyphosphoinositides (15, 16).

To probe the molecular basis of phosphoinositide interactions, we solved the structure of the NH₂-terminal domain from the close AP180 homolog, CALM, at 2 Å resolution (19, 20) (crystals of AP180-N did not diffract well). There were nine α helices forming a solenoid structure (Fig. 2). This is reminiscent of other protein families formed from a superhelix of α helices such as the armadillo (21) and tetratricopeptide repeat (22) domains, but it is most similar to the ENTH domain of epsin (23) (Fig. 2B). The first seven helices of epsin superimposed well on those of CALM. In epsin, however, the final α 8 helix folded back across the others, whereas in CALM the final three long helices continued the solenoidal pattern. Because of the high sequence homology of CALM-N and AP180-N (81% sequence identity) (Fig. 2), we can safely assume that the NH₂-terminal domain of AP180 has the same structure.

X-ray data were collected at 2 Å resolution from CALM-N crystals soaked in a series of inositol phosphates and phospholipids. Binding was observed for inositol hexakisphosphate (D-myo-inositol-1,2,3,4,5,6-hexakisphosphate, InsP₆), inositol-4,5-bisphosphate [Ins(4,5)P₂], and a soluble short-chain (diC₈) L- α -D-myo-phosphatidylinositol-4,5-bisphosphate. No significant binding was observed in the crystal for short-chain (diC₈) L- α -D-myo-phosphatidylinositol-3,4,5-trisphosphate. The binding site is unusual (Fig. 2): Typical ligand-binding sites on proteins lie in a pocket or groove, but this site is on the surface, with the phosphates perched on the tips of the side chains of three lysines and a histidine, like a ball balanced on the fingertips. In all ligands, only the two phosphates were well ordered and contacted the protein. The cluster of lysines and histidine formed a marked positively charged patch on the surface (Fig. 2C), appropriate for a phosphate-binding protein.

Database searches with the AP180-N/CALM-N identified several classes of related sequences (Fig. 2H). First, there were the members of the AP180 family itself, with a conserved NH₂-terminal domain, having PtdIns(4,5)P₂-binding motifs, which we identified from the observed binding in the crystal, K(X)₃KX(K/R)(H/Y). The COOH-terminal domains of these proteins contain clathrin-binding motifs (3, 24), as well as Asp-Pro-Phe (DPF)-like α - and β -adaptin-

Medical Research Council (MRC) Laboratory of Molecular Biology, Hills Road, Cambridge, CB2 2QH, UK.

*MRC Laboratory of Molecular and Cell Biology, University College London, Gower Street, London, WC1E 6BT, UK.

†To whom correspondence should be addressed. E-mail: pre@mrc-lmb.cam.ac.uk, hmm@mrc-lmb.cam.ac.uk

REPORTS

binding motifs (7, 25) and Asn-Pro-Phe (NPF) motifs, which bind to Eps15 homology (EH) domains (26) (see Fig. 1A). Second, there were other proteins similar to AP180, containing the PtdIns(4,5)P₂-binding motifs, but having unrelated COOH-terminal regions. Of these proteins, Huntingtin interacting protein 1 (HIP1) and SLA2p have actin-binding regions in their COOH-termini. Third, there were the epsin-related proteins; these showed a lower sequence homology in the NH₂-terminus but shared the same structure for at least the first 140 residues (Fig. 2). They lack completely the PtdIns(4,5)P₂-binding motif, but have a signature (D/E)PW motif in the loop connecting α1 to α2. According to our predictions, α-adaptin (which has no sequence homology to AP180) has a PtdIns(4,5)P₂-binding motif near its NH₂-terminus between the first two predicted helices. Indeed, a fragment from this region of the protein has been shown to bind PtdIns(4,5)P₂ (4).

Specificity of the phosphoinositide interaction with AP180-N and CALM-N was tested by sedimentation assays using liposomes or lipid tubules (19, 27, 28). Tubules containing 10% PtdIns(4,5)P₂ efficiently sedimented AP180-N and CALM-N with the same apparent affinity (K_M values of $4.6 \pm 0.7 \mu\text{M}$ and $5.8 \pm 1.7 \mu\text{M}$, respectively) but mutations in the PtdIns(4,5)P₂ motif (KKK-EEE) abolished sedimentation (Fig. 3A). AP180-N was likewise sedimented with liposomes containing 10% PtdIns(4,5)P₂, but not with liposomes when replaced with 10% phosphatidylserine (PtdSer), or 10% PtdIns, or 10% PtdIns(3,4)P₂ and less efficiently with liposomes containing 10% PtdIns(4)P or 10%

PtdIns(3,5)P₂ or 10% PtdIns(3,4,5)P₃ (Fig. 3B). Full-length AP180 binds to lipid tubules or liposomes containing PtdIns(4,5)P₂ with characteristics similar to those of AP180-N; however, a mutant in the PtdIns(4,5)P₂-binding motif (KKK-EKE) does not (Fig. 3C).

Combinations of full-length AP180, AP2, and clathrin were then tested in sedimentation assays with PtdIns(4,5)P₂-containing liposomes. AP2 was sedimented both in the presence and absence of AP180 (Fig. 3C). Clathrin only sedimented in the presence of AP180 [but not the PtdIns(4,5)P₂-bind-

ing motif mutant], and then it associated preferentially with the lipid-bound AP180. Incubation of AP180, AP2, and clathrin resulted in the sedimentation of all components, and the clathrin in the pellet was resistant to 1% Triton X-100 treatment, implying a degree of polymerization (addition of Triton X-100 has been used as a purification step in the isolation of clathrin coats). Specificity of sedimentation was confirmed by using a number of controls including the absence of liposomes (Fig. 3C).

Fig. 1. Overexpression of AP180 in COS-7 cells inhibits endocytosis. (A) Domain structure of AP180 and other family members; red boxed regions (with annotated sequence identities) indicate the conserved domain homology. The strongest predicted clathrin-binding site is indicated (orange), but other sites are present, at least in AP180 and CALM. **(B)** Immunofluorescence data of EGF (green) uptake in cells transiently transfected with AP180, AP180-N, or AP180-C (stained red). The panel immediately below AP180-C is the same field stained for endogenous distribution (white). **(C)** Electron microscopy of immunogold-labeled transferrin receptors (arrows) in COS-7 cells transiently transfected with AP180-C. Transferrin receptors no longer accumulated in coated pits. WT, wild type.

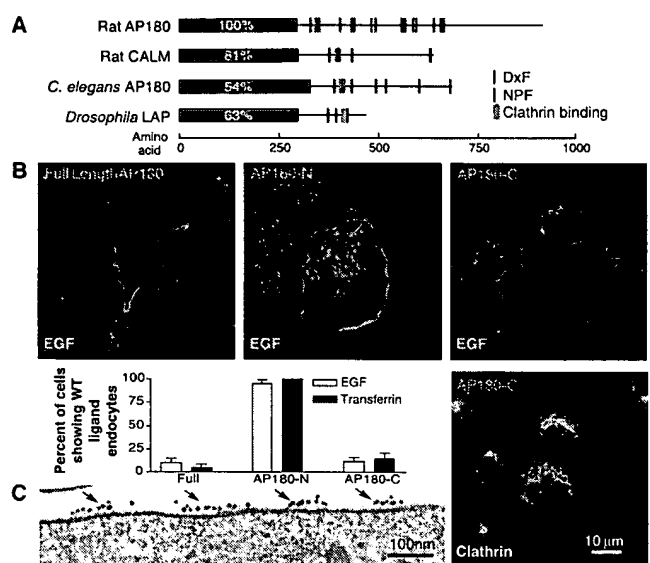


Table 1. Crystallographic statistics. Values in parentheses apply to the high-resolution shell.

	Native	EMTS	PtdIns(4,5)P ₂	Ins(4,5)P ₂	InsP ₆
Data collection					
Resolution (Å) (outer bin)	2.0 (2.11)	2.0 (2.11)	2.0 (2.11)	2.0 (2.11)	2.0 (2.11)
R_{merge}^*	0.080 (1.036)	0.124 (2.03)	0.104 (1.153)	0.126 (1.958)	0.082 (0.952)
R_{meas}^\dagger	0.083 (1.077)	0.145 (2.39)	0.112 (1.468)	0.136 (2.113)	0.088 (1.033)
Completeness (%)	100 (100)	100 (100)	100 (100)	99.4 (99.9)	100 (100)
Multiplicity	14.0 (13.3)	6.9 (6.7)	7.1 (7.0)	7.2 (7.0)	7.0 (6.4)
Wilson plot B (Å ²)	43	43	43	43	44
Refinement					
R ($R_{\text{free}}^{\ddagger}$)	0.187 (0.220)		0.195 (0.230)	0.193 (0.215)	0.190 (0.219)
$\langle B \rangle$ (Å ²)	48		49	49	49
$N_{\text{reflections}} (N_{\text{free}})$	26,057 (1,324)		26,014 (1,322)	25,847 (1,315)	25,815 (1,310)
$N_{\text{atoms}} (N_{\text{water}})$	2,244 (130)		2,289 (128)	2,282 (128)	2,278 (128)
R_{msd} bond length (Å)	0.031		0.032	0.026	0.031
R_{msd} bond angle (°)	2.1		2.5	2.2	2.4
Number of Ramachandran violations	0	0	0	0	0
MIR phasing		EMTS			
Number of sites		2 (one of them split)			
R_{deriv}^{\S}		0.16			
$R_{\text{cullis}}^{\parallel}$ (centric, acentric)		0.63, 0.74			
Phasing power: isomorphous (anomalous) ¶		1.35 (0.70)			
Mean figure of merit		0.59			
Figure of merit after solvent flattening (all data)		0.91*			

* $R_{\text{merge}} = \sum_i |I_h - \langle I_h \rangle| / \sum_i I_h$, where I_h is the mean intensity for reflection h . $^\dagger R_{\text{meas}} = \sqrt{(n/n-1) \sum_i |I_h - \langle I_h \rangle| / \sum_i I_h}$, the multiplicity weighted R_{merge} . $^\ddagger R = \sum_i |F_p - F_{\text{calc}}| / \sum_i F_p$. $^\S R_{\text{deriv}} = \sum_i |F_{\text{PH}} - F_p| / \sum_i F_p$. $^\parallel R_{\text{cullis}} = \sum_i |F_{\text{PH}} - F_p| - |F_{\text{H(calc)}}| / \sum_i |F_{\text{PH}} - F_p|$. ¶ Phasing power = $\langle |F_{\text{H(calc)}}| \rangle / \text{phase-integrated lack of closure}$.

REPORTS

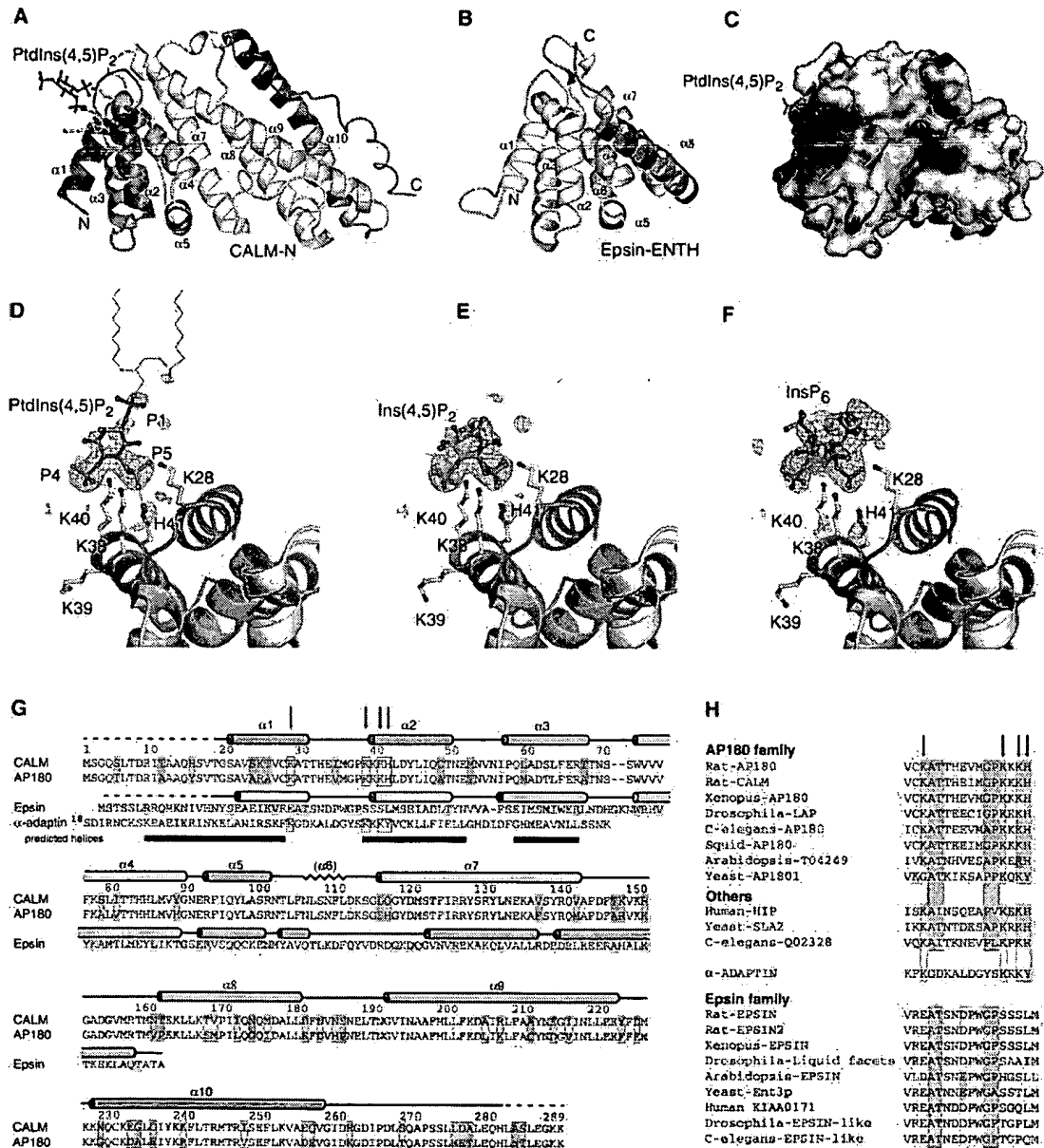
The recruitment of clathrin by AP180 was further investigated by electron microscopy to visualize clathrin lattice and cage formation. In the presence of AP180 and clathrin, latticelike structures formed on the surface of lipid monolayers (29) (Fig. 4A). Addition of AP2 resulted in the formation of more distinct electron-dense areas of clathrin assembly (Fig. 4B). Single-angle platinum shadowing of negatively stained grids showed that in the absence of AP2 the lattice was predominantly flat (Fig. 4C). Invaginated coated buds were

formed in the presence of AP2 (Fig. 4D). The diameter was well within the expected size range for brain-derived coated vesicles. In the absence of AP180, no detectable intermediates were visible by electron microscopy. When PtdIns(4,5) P_2 was replaced by PtdIns, the flat clathrin lattices were no longer seen (Fig. 4E).

Our experiments demonstrate that the minimal requirements for the initial stage of coated pit invagination are clathrin, AP180, AP2, and PtdIns(4,5) P_2 -containing membranes. However, with these compo-

nents, the pits do not invaginate completely, even in the presence of excess clathrin. AP180 concentrates clathrin on the membrane, and AP2s stimulate curved lattice assembly, consistent with their coat assembly activity (6). On a more general note, we show that the AP180 NH_2 -terminal domain is a PtdIns(4,5) P_2 -binding domain responsible for membrane localization of AP180, and we propose that similar domains found in other proteins will also recruit them specifically to PtdIns(4,5) P_2 -rich membranes.

Fig. 2. The structure of CALM-N bound to PtdIns(4,5) P_2 . (A) Ribbon diagram of CALM-N, colored from green at the NH_2 -terminus to gold at the COOH-terminus. (B) The ENTH domain of epsin in the same orientation [PDB code 1edu (23)]. (C) The surface of CALM-N colored by electrostatic potential, red +10 kT e^{-1} , blue -10 kT e^{-1} . This is a slightly different view from that in (A), to show the strong positive patch that binds PtdIns(4,5) P_2 . (D) Close-up of PtdIns(4,5) P_2 -binding site, showing a difference electron density map omitting the ligand, contoured at 2 σ . There was strong density only for the 4- and 5-phosphates, weak density for the inositol ring and the 1-phosphate, and none for the lipid chains. (E) Ins(4,5) P_2 also shows most density for the phosphates: it was modeled as a 50:50 mixture of two binding modes interchanging the 4- and 5-phosphates. (F) Ins P_6 was probably bound in multiple orientations, and the orientation of the inositol ring was different from that of the bisphosphates. (G) Sequence alignments of the very similar CALM-N and AP180-N (81% identical, unshaded, further conserved residues shaded mauve), and the structurally similar epsin ENTH domain (16% sequence identity, shaded orange). α Helices are shown as cylinders, colored as in A and B. PtdIns(4,5) P_2 -binding residues are marked with arrows. Also shown is the PtdIns(4,5) P_2 -binding region of α -adaptin, with the conserved PtdIns(4,5) P_2 -binding motif and predicted α helices. (H) The $\alpha 1$ to $\alpha 2$ loop regions for three families of proteins:



AP180/CALM family with the PtdIns(4,5) P_2 -binding motif (blue); some other proteins with the PtdIns(4,5) P_2 -binding motif (blue); epsin family with the (D/E)PW motif (orange). Other conserved residues are colored purple. Yeast-SLA2 is Yeast-SLA2p.

REPORTS

Fig. 3. AP180-N binds, and has specificity for, PtdIns(4,5)P₂. (A) AP180-N and CALM-N are sedimented by lipid tubules containing 10% PtdIns(4,5)P₂. The measurements on the abscissa refer to the amount of PtdIns(4,5)P₂ in the experiment; the amount of tubules is therefore 10 times this value. Each assay contained 0.05 mg/ml protein. (B) Liposomes containing 10% cholesterol, 40% phosphatidylethanolamine, 40% phosphatidylcholine, and 10% of a test lipid were prepared and used to evaluate the lipid specificity of AP180-N. Each experiment contained 0.05 mg/ml protein and 50 μ M of the lipid under investigation; each experiment, therefore, contained a total lipid concentration of 500 μ M. (C) AP180 recruits clathrin to PtdIns(4,5)P₂ containing liposomes (27). Pellets (P) and supernatants (S) were separated by centrifugation. In AP180mut, lysines 38 and 40 were changed to glutamic acids. Although AP2 alone sedimented approximately as efficiently as AP180, it was not capable of sedimenting together with clathrin, possibly because of a requirement for cargo and/or oligomerization. Averages of at least three experiments are shown in the bar graph. Experiments contained 0.05 mg/ml AP180, 0.05 mg/ml AP2, 0.025 mg/ml clathrin in a final volume of 100 μ l. All gels were stained with Coomassie Blue.

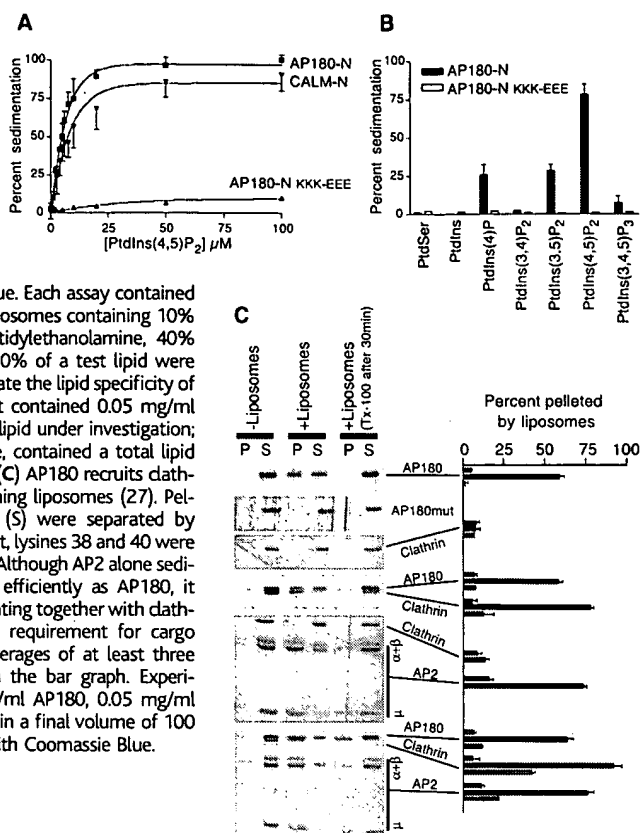
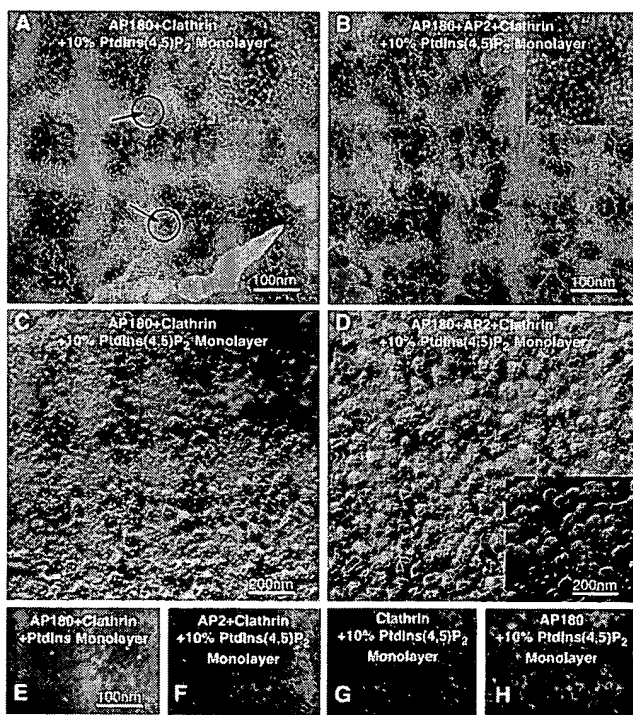


Fig. 4. Clathrin recruitment to lipid monolayers by AP180. (A) AP180, when incubated with clathrin in the presence of lipid monolayers recruited clathrin to the monolayer surface and promoted lattice assembly. The presence of a few pentagons among hexagons and the spherical outlines imply the beginning stages of coated pit invagination. The lattices formed had a diameter of 66 ± 7 nm. (B) The presence of AP180, AP2, and clathrin resulted in the formation of cages with electron-dense cores, which appeared deeply invaginated. The diameter of the cages thus formed was 77 ± 9 nm. Cracked areas lack cages. These experiments also worked on brain Folch lipids. (C and D) Single-angle platinum-shadowed monolayers showed that the clathrin assemblies were budded from the lipid surface in the presence of AP2 (inset: rotary platinum shadowing). We have shown more dense area of the grids compared with the negatively stained panels. (E to H) Controls showed no evidence of clathrin assemblies.



Note added in proof: It has been reported (44) that AP180 and its clathrin-binding domain inhibit transferrin endocytosis in HeLa and Cos cells and redistribute endogenous clathrin in HeLa cells.

References and Notes

1. J. Hirst, M. S. Robinson, *Biochim. Biophys. Acta* **1404**, 173 (1998).
2. M. Marsh, H. T. McMahon, *Science* **285**, 215 (1999).
3. T. Kirchhausen, *Annu. Rev. Biochem.* **69**, 699 (2000).
4. I. Gaidarov, J. H. Keen, *J. Cell Biol.* **146**, 755 (1999).
5. T. Kirchhausen, *Annu. Rev. Cell Dev. Biol.* **15**, 705 (1999).
6. D. J. Owen, Y. Vallis, B. M. Pearce, H. T. McMahon, P. R. Evans, *EMBO J.* **19**, 4216 (2000).
7. The α and β appendage domains of the AP2 adaptor complex bind to cytoplasmic proteins with DPF-like motifs (Asp-Pro-Phe) (6, 30, 31). These proteins include AP180, amphiphysin, EPS15, epsin, and auxilin—all proteins known to function in clathrin-mediated endocytosis.
8. R. Lindner, E. Ungewickell, *J. Biol. Chem.* **267**, 16567 (1992).
9. S. A. Morris, S. Schroder, U. Plessmann, K. Weber, E. Ungewickell, *EMBO J.* **12**, 667 (1993).
10. W. Ye, N. Ali, M. E. Bembek, S. B. Shears, E. M. Lafer, *J. Biol. Chem.* **270**, 1564 (1995).
11. H. T. McMahon, *Curr. Biol.* **9**, R332 (1999).
12. B. Zhang et al., *Neuron* **21**, 1465 (1998).
13. M. L. Nonet et al., *Mol. Biol. Cell* **10**, 2343 (1999).
14. M. H. Dreyling et al., *Proc. Natl. Acad. Sci. U.S.A.* **93**, 4804 (1996).
15. F. A. Norris, E. Ungewickell, P. W. Majerus, *J. Biol. Chem.* **270**, 214 (1995).
16. W. Hao et al., *J. Biol. Chem.* **272**, 6393 (1997).
17. cDNAs encoding full-length AP180 and AP180-C (residues 530 to 915) were cloned into pCMV-MYC for expression in COS-7 cells. AP180-N (residues 1 to 289) was cloned into pcDNA. Clathrin-mediated endocytosis was measured by assaying EGF and transferrin uptake (32) on an MRC 1024 confocal microscope. Antibodies used for immunofluorescence are as follows: A14 (MYC-tag), Ra24 (AP180-N), and X-22 (clathrin), and secondary antibodies were conjugated with Texas Red or Cy-5. Transfected cells were compared with untransfected controls in their immediate vicinity. Blocked cells were defined as those transfected cells in which EGF or transferrin uptake was <20% that of untransfected controls. Blocked cells were expressed as a percentage of the total number of transfected cells, sampled in multiple fields and in multiple separate experiments. For immunoelectron microscopy of fibroblasts, cells either expressing the human transferrin receptor alone (cloned into pRK5), or coexpressing this with AP180-C were incubated at 4°C with B3/25 (antibody against human transferrin) conjugated to 10 nm gold for 90 min, rinsed, fixed, and processed as described (33). Sections were analyzed morphometrically by using standard techniques.
18. F. Tebar, S. K. Bohlander, A. Sorkin, *Mol. Biol. Cell* **10**, 2687 (1999).
19. AP180-N and CALM-N (residues 1 to 289) and mutants thereof were expressed as NH₂-terminal glutathione S-transferase fusion proteins in BL21 cells. Protein was expressed overnight at 22°C and purified from extracts by passage over a glutathione-agarose column. The protein was cleaved with thrombin in 20 mM Hepes, pH 7.4, 150 mM NaCl, and 4 mM dithiothreitol (DTT). AP180-N and CALM-N were purified further by passage over Q-Sepharose followed by S200 gel filtration. For crystallization trials, AP180-N was concentrated to 40 mg/ml and CALM-N was concentrated to 16 mg/ml. For sedimentation assays, protein was typically used at 1 mg/ml. Full-length His₆-tagged rat brain AP180 was purified from baculovirus-infected Sf9 cells 48 hours after infection. Protein was purified on a Ni-nitrilotriacetic acid (Ni-NTA) column, dialyzed into 20 mM Hepes, pH 7.4, 75 mM NaCl, and 4 mM DTT with protease inhibitors and bound to a Q-Sepharose column. Protein was eluted using a NaCl gradient from 75 to 300 mM.

REPORTS

- After concentration, the protein was passed through an S200 gel filtration column, using running buffer (20 mM Hepes, pH 7.4, 150 mM NaCl, 4 mM DTT). Clathrin and AP2 were purified from fresh pig brain as previously described (34). AP2 was dialyzed against 50 mM triethanolamine-KCl, pH 8.0, 200 mM NaCl, 0.2 mM EDTA, 0.1% β -mercaptoethanol, and 0.02% NaN_3 . Clathrin cage formation was performed as described previously (6) in 25 mM Hepes, 125 mM K acetate, and 1 mM Mg acetate, pH 7.4.
20. Crystals of CALM-N (residues 1 to 289) were grown in seeded hanging drops against a reservoir containing 0.1 M Hepes, pH 7.5, 12 to 14% PEG 8000, and 8% ethylene glycol. They belong to space group $P4_22_1$, cell dimensions $a = b = 77.93$ Å, $c = 121.81$ Å, with one molecule per asymmetric unit. For the binding studies, crystals were soaked for 1 hour in 1 mM ligand in 0.1 M Hepes, pH 7.5, 14% PEG 8000, and 8% ethylene glycol. We were unable to find suitable conditions for cryoprotection, so all data sets were collected at room temperature from crystals mounted in capillaries, on beamline 9.6 at SRS Daresbury, $\lambda = 0.88$ Å. By setting the ADSC Quantum 4 charge-coupled device detector to the fastest readout time (~ 3 s) and using a 3-s exposure for a 1° rotation, a 90° data set could be collected in less than 10 min with acceptable radiation damage. Images were integrated using Mosflm (35) and scaled using CCP4 programs (36). All data sets extended to 2 Å resolution and were reasonably strong to 2.1 Å resolution (see PDB depositions and Table 1 for details). Phases were derived from a single mercury derivative with two sites (crystals soaked for 1 hour in 1 mM ethylmercury thiosalicylate) by the program Sharp (37). Solvent flattening with Solomon led to an easily interpretable map. The model was built using O (38) and refined using Refmac5 (39). The termini (1 to 19 and 281 to 289) were not visible. Density was weak around the $\alpha 7$ to $\alpha 8$ loop (149 to 165); around the $\alpha 9$ to $\alpha 10$ loop (215 to 237); and the COOH-terminal region from about 267. Final R factors for the native and complexes were 0.187 to 0.195 (R_{free} 0.215 to 0.230). Coordinates have been deposited in the PDB with access codes 1hf8 (native), 1hfa [PtdIns(4,5) P_2], 1hg2 [Ins(4,5) P_2], and 1hg5 [Ins P_6].
 21. E. Conti, M. Uy, L. Leighton, G. Blobel, J. Kuriyan, *Cell* **94**, 193 (1998).
 22. A. K. Das, P. W. Cohen, D. Barford, *EMBO J.* **17**, 1192 (1998).
 23. J. Hyman, H. Chen, P. P. Di Fiore, P. De Camilli, A. T. Brunger, *J. Cell Biol.* **149**, 537 (2000).
 24. E. C. Dell'Angelica, J. Klumperman, W. Stoorvogel, J. S. Bonifacio, *Science* **280**, 431 (1998).
 25. Single-letter abbreviations for the amino acid residues are as follows: A, Ala; C, Cys; D, Asp; E, Glu; F, Phe; G, Gly; H, His; I, Ile; K, Lys; L, Leu; M, Met; N, Asn; P, Pro; Q, Gln; R, Arg; S, Ser; T, Thr; V, Val; W, Trp; X, any amino acid; and Y, Tyr.
 26. T. de Beer, R. E. Carter, K. E. Lobel-Rice, A. Sorkin, M. Overduin, *Science* **281**, 1357 (1998).
 27. Lipid tubules [10% PtdIns(4,5) P_2 , 10% cholesterol, 40% phosphatidylcholine, 40% NFA-galactocerebrosides type II] were prepared as described in (40). Liposomes [10% PtdIns(4,5) P_2 , 10% PtdSer, 10% cholesterol, 35% phosphatidylcholine, and 35% phosphatidylethanolamine] were prepared by evaporating solvent from an appropriate mixture of lipids under a constant stream of argon. After resuspension in 10 mM Hepes, pH 7.4, the mixtures were extruded through a filter with pore size 0.1 μm . Initially, tubules were used for comparison with our studies on dynamin, whose pleckstrin homology domain binds phosphoinositol head groups (40). Moreover, tubules are easier to sediment than liposomes. Dynamin was also used in the liposome experiments as a positive control for the incorporation of phosphatidyl inositols.
 28. Protein(s) and liposomes or tubules (as appropriate) were added to reaction buffer (25 mM Hepes, pH 7.4, 125 mM K acetate, 1 mM Mg acetate) in a polycarbonate centrifuge tube (final volume of each experiment 50 or 100 μl). Experiments were incubated at room temperature for 30 min before sedimentation by centrifugation (78,000g for 20 min in a TLA100 rotor) and analyzed by Coomassie-stained gels. Densitometry was carried out using a Molecular Dynamics scanner and bands were integrated using ImageQuant for Macintosh v1.2.
 29. A monolayer of lipid [same composition as 10% PtdIns(4,5) P_2 liposomes] was formed on the surface of a buffer droplet in a Teflon block (41), and the protein(s) of interest were introduced into the buffer. After 5 min, a carbon-coated gold electron microscopy grid was placed onto the monolayer. After 1 hour, the grid was removed and stained with uranyl acetate (2% uranyl acetate, 0.0025% polyacrylic acid). The technique has been used for the generation of two-dimensional crystals (41, 42) and, to our knowledge, has not been applied to study the formation of endocytic intermediates. Potassium in the buffer was critical for the efficient polymerization of clathrin in keeping with previous observations (43).
 30. D. J. Owen et al., *Cell* **97**, 805 (1999).
 31. L. M. Traub, M. A. Downs, J. L. Westrich, D. H. Fremont, *Proc. Natl. Acad. Sci. U.S.A.* **96**, 8907 (1999).
 32. P. Wigge, Y. Vallis, H. T. McMahon, *Curr. Biol.* **7**, 554 (1997).
 33. C. E. Futter, A. Pearce, L. J. Hewlett, C. R. Hopkins, *J. Cell Biol.* **132**, 1011 (1996).
 34. C. J. Smith, N. Grigoriou, B. M. Pearce, *EMBO J.* **17**, 4943 (1998).
 35. A. G. W. Leslie, in *Joint CCP4 and ESF-EACMB Newsletter on Protein Crystallography* No. 26 (SERC, Daresbury Laboratory, Warrington, UK, 1992).
 36. Collaborative Computational Project No. 4, *Acta Crystallogr.* **D50**, 760 (1994).
 37. E. de la Fortelle, G. Bricogne, *Methods Enzymol.* **276**, 472 (1997).
 38. T. A. Jones, J. Y. Zou, S. W. Cowan, M. Kjeldgaard, *Acta Crystallogr.* **A47**, 110 (1991).
 39. G. N. Murshudov, A. A. Vagin, E. J. Dodson, *Acta Crystallogr.* **D53**, 240 (1997).
 40. M. H. Stowell, B. Marks, P. Wigge, H. T. McMahon, *Nature Cell Biol.* **1**, 27 (1999).
 41. D. Levy et al., *J. Struct. Biol.* **127**, 44 (1999).
 42. R. D. Kornberg, S. D. Darst, *Curr. Opin. Struct. Biol.* **1**, 642 (1991).
 43. J. E. Heuser, R. G. Anderson, *J. Cell Biol.* **108**, 389 (1989).
 44. X. Zhao et al., *J. Cell Sci.* **114**, 353 (2001).
 45. We thank O. Perisic for advice on liposome preparation, E. Ungewickell for the AP180 clone, L. Serpell and J. Berriman for assistance with platinum shadowing, D. Brodersen and B. Clemons for assistance with data collection, and the staff of beamline 9.6, SRS Daresbury. Also, we thank N. Unwin and members of our labs for extensive discussion.

20 November 2000; accepted 18 December 2000

Notch Inhibition of RAS Signaling Through MAP Kinase Phosphatase LIP-1 During *C. elegans* Vulval Development

Thomas Berset, Erika Fröhli Hoier, Gopal Battu, Stefano Canevascini, Alex Hajnal*

During *Caenorhabditis elegans* vulval development, a signal from the anchor cell stimulates the RTK/RAS/MAPK (receptor tyrosine kinase/RAS/mitogen-activated protein kinase) signaling pathway in the closest vulval precursor cell P6.p to induce the primary fate. A lateral signal from P6.p then activates the Notch signaling pathway in the neighboring cells P5.p and P7.p to prevent them from adopting the primary fate and to specify the secondary fate. The MAP kinase phosphatase LIP-1 mediates this lateral inhibition of the primary fate. LIN-12/NOTCH up-regulates *lip-1* transcription in P5.p and P7.p where LIP-1 inactivates the MAP kinase to inhibit primary fate specification. LIP-1 thus links the two signaling pathways to generate a pattern.

MAP kinase phosphatases (MKPs) belong to the family of dual-specificity phosphatases that inactivate different types of MAP kinases by dephosphorylating the critical phosphotyrosine and phosphothreonine residues of the kinases (1). The transcription

of MKPs is rapidly induced by various stimuli such as growth factors and cellular stresses that activate MAP kinases, suggesting that MKPs may participate in an autoinhibitory feedback loop.

To study the role of MKPs in RTK/RAS/MAPK signaling during development, we searched the *C. elegans* genome sequence for homologs of vertebrate MKPs. Among the 185 predicted phosphatases, we identified a candidate, termed *lip-1* (lateral signal induced phosphatase—1, open read-

Division of Cancer Research, Department of Pathology, University of Zürich, Schmelzbergstrasse 12, CH-8091 Zürich, Switzerland.

*To whom correspondence should be addressed. E-mail: ahajnal@pathol.unizh.ch

Serum Antibodies to Huntingtin Interacting Protein-1: A New Blood Test for Prostate Cancer

Sarah V. Bradley,¹ Katherine I. Oravec-Wilson,¹ Gaelle Bougeard,¹ Ikuko Mizukami,¹ Lina Li,¹ Anthony J. Munaco,¹ Arun Sreekumar,² Michael N. Corradetti,¹ Arul M. Chinnaiyan,^{2,3} Martin G. Sanda,³ and Theodora S. Ross¹

Departments of ¹Internal Medicine, ²Pathology, and ³Urology, University of Michigan Medical School, Ann Arbor, Michigan

Abstract

Huntingtin-interacting protein 1 (HIP1) is frequently overexpressed in prostate cancer. HIP1 is a clathrin-binding protein involved in growth factor receptor trafficking that transforms fibroblasts by prolonging the half-life of growth factor receptors. In addition to human cancers, HIP1 is also overexpressed in prostate tumors from the transgenic adenocarcinoma of the mouse prostate (TRAMP) mouse model. Here we provide evidence that HIP1 plays an important role in mouse tumor development, as tumor formation in the TRAMP mice was impaired in the *Hip1*^{null/null} background. In addition, we report that autoantibodies to HIP1 developed in the sera of TRAMP mice with prostate cancer as well as in the sera from human prostate cancer patients. This led to the development of an anti-HIP1 serum test in humans that had a similar sensitivity and specificity to the anti- α -methylacyl CoA racemase (AMACR) and prostate-specific antigen tests for prostate cancer and when combined with the anti-AMACR test yielded a specificity of 97%. These data suggest that HIP1 plays a functional role in tumorigenesis and that a positive HIP1 autoantibody test may be an important serum marker of prostate cancer. (Cancer Res 2005; 65(10): 4126-33)

Introduction

Currently, the prostate-specific antigen (PSA) blood test is widely relied upon for the early detection of prostate cancer. Despite the fact that this test was identified almost 20 years ago and standardized >10 years ago (1), the effect of this screening on mortality is not yet defined (2-4) and both its sensitivity (5, 6) and specificity (7) have limitations. Although there has been a stage migration with the use of the PSA test and therefore this test likely diminishes mortality from prostate cancer, the discovery of new biomarkers for early diagnosis and prognosis of prostate cancer may improve management of and survival from prostate cancer.

Recently, the identification of a test that identifies autoantibodies to the prostate tumor marker, α -methylacyl CoA racemase (AMACR) provided hope that use of cytoplasmic tumor markers in addition to secreted antigens could lead to blood screening tests (8). The proposed reason for the formation of autoantibodies is that upon turnover of tumor cells, tumor antigens are shed into the circulation at low levels inducing an

immune response. Immunoreactivity to other cytoplasmic tumor antigens has been described in prostate cancer patients previously, but the formation of these autoantibodies did not show high sensitivities (9-11).

Because HIP1 is specifically up-regulated in prostate cancer relative to benign prostatic epithelia (12) and is a cytoplasmic protein, we hypothesized that HIP1 autoantibody formation could, like AMACR, yield a useful blood test for prostate cancer. In addition, because overexpression of HIP1 is associated with advanced prostate cancer (12) and HIP1 directly transforms fibroblasts (13), we hypothesized that HIP1 may be necessary for *in vivo* tumor cell survival or progression.

To experimentally evaluate these two questions in mice, we employed the transgenic adenocarcinoma of the mouse prostate (TRAMP) model (14) and *Hip1* mutant mice generated in our laboratory (15). TRAMP mice express SV40 T antigen under the control of the *probasin* promoter. This targets transgene expression to the epithelial cells of the prostate and leads to prostate cancer. Although many of the tumors in these mice are more representative of a neuroendocrine rather than epithelial cancer (16), the progression of these cancers in the TRAMP model is similar to human prostate cancer in that the prostates of these mice develop hyperplastic epithelia, *in situ* carcinoma, locally invasive cancers followed by metastases to the liver, lung, lymph nodes, and bone. In addition to providing evidence here that HIP1 may indeed be necessary for tumorigenesis in the TRAMP prostate, we have discovered that both TRAMP mice and men with prostate cancer produce autoantibodies to HIP1 more frequently than control individuals. Using both immunoblot and ELISA tests, described herein, we have found that the sensitivity and specificity of this novel prostate cancer blood test is similar to that of PSA, and when combined with AMACR, has the exciting potential to surpass the specificity of the PSA test.

Materials and Methods

Animals. The *Hip1*^{null/null} mice (15) and TRAMP mice (14) were maintained on a C57BL/6;129svj and C57BL/6 background, respectively. SV40 T antigen "homozygous" TRAMP male mice were intercrossed with *Hip1*^{null/null} females to generate T antigen transgenic (TRAMP) mice that were heterozygous for the *Hip1* mutation (TRAMP/*Hip1*^{null/+}). The latter mice were intercrossed to make TRAMP littermates containing either wild type or knockout *Hip1* alleles. Mouse tail DNA was genotyped for the SV40 T antigen by PCR (14) or for the *Hip1* null allele by Southern (15, 17). Euthanized mice were subjected to complete necropsy as well as *Hip1*/SV40 T antigen genotype verification via repeat southern blot of tail tissue and Western blot of tumors for the presence or absence of HIP1 and T antigen proteins. Mouse care followed established institutional guidelines.

Evaluation of transgenic adenocarcinoma of the mouse prostate tissue. Sixteen TRAMP/*Hip1*^{+/-} and eight TRAMP/*Hip1*^{null/null} littermate mice were analyzed for tumor extent at 6.5 months of age. Prostate and

Note: S.V. Bradley and K.I. Oravec-Wilson contributed equally to this work.

Requests for reprints: Theodora S. Ross, University of Michigan, 6322 CCGC, 1500 East Medical Center Drive, Ann Arbor, MI 48109-0942. Phone: 734-615-5509; E-mail: tsross@umich.edu.

©2005 American Association for Cancer Research.

Table 1. Clinical data for prostate cancer patients used in study

Characteristic	Value
Mean age (y) \pm SD*	59.0 \pm 8.0
Mean gland size (cm) \pm SD†	1.6 \pm 1.5
Mean gland weight (g) \pm SD‡	53.6 \pm 51.8
PSA§ (%)	
Mean \pm SD (ng/mL)	7.5 \pm 5.9
<4 ng/mL	23.3
4-10 ng/mL	55.5
>10 ng/mL	21.1
Biochemical recurrence	10.0
Gleason grade \leq 6 (%)§	38.9
Gleason grade \geq 7 (%)§	60.1

*Data were available for 91 patients only.

†Data available for 89 patients.

‡Data available for 97 patients.

§Data available for 90 patients.

tumor samples were fixed in 10% (v/v) buffered formalin, embedded in paraffin, serially sectioned and stained by H&E. The slides of prostatic tissue were evaluated for the presence of hyperplasia, adenoma, or invasive adenocarcinoma as described previously (18).

Acquisition of serum samples from transgenic adenocarcinoma of the mouse prostate mice. TRAMP mice and T antigen-negative control mice were initially bled between the ages of 2 and 4 months from the saphenous vein of the hind leg. Approximately 100 to 200 μ L of blood was collected into Microvette CB 300 serum separation tubes (Starstadt, Nümbrecht, Germany) and 30- to 40- μ L aliquots were stored at -20°C until analyzed.

Human patient cohort and samples. This study was approved by the University of Michigan Medical School Institutional Review Board. At the time of diagnosis and before prostatectomy, sera from 97 biopsy-proven clinically localized prostate cancer patients were collected and stored in the University of Michigan Prostate Specialized Programs of Research Excellence Tissue/Serum Bank from January 1995 to January 2003. The average age of the participants was 59 (range, 41-83). Table 1 summarizes the clinical data for the 97 prostate cancer patients. As controls, sera from 211 male subjects (average age, 61; range, 29-84; collected at the University of Michigan clinical pathology laboratories from May 2001 to May 2003) with no known history of cancer were used. All sera were stored in aliquots at -20°C .

Preparation of HIP1 antigen. A glutathione S-transferase-3'HIP1 (GST-3'HIP1) fusion construct was used to generate 3'HIP1 antigen. Briefly, GST was fused in frame to the COOH-terminal half of HIP1 amino acid sequence starting at the sole internal *Eco*RI site (nucleotide 1250) and ending at the native stop codon (nucleotide 3010; ref. 19). Expression of antigen was induced in bacteria with 0.1 mmol/L isopropyl-L-thio-B-D-galactopyranoside for 4 hours at 37°C , bacteria were sonicated and antigen initially fractionated from other bacterial proteins with glutathione-Sepharose. GST was then cleaved off of the partially pure protein with thrombin. The antigen was separated from free GST on a preparative 8% SDS-PAGE gel, electroeluted, dialyzed, and concentrated to obtain further purity.

Immunoblot analysis of anti-HIP1 antibodies in mouse or human serum. 3'HIP1 protein (10 μ g for mouse sera and 20 μ g for human sera) was separated on a 10% preparative gel, transferred to nitrocellulose, and blocked overnight at 4°C in TBST (mouse sera) or TBS (human sera) with 5% milk and 5% goat (mouse samples) or donkey (human samples) serum ("blocking solution"). A Miniblotter 28-dual unit system (Immunetics, Inc., Cambridge, MA) was used to make 25 incubation chambers for serum samples, diluted 1:50 in 1:10 blocking solution (human sera) or 1:15 in

TBST/5% milk (mouse sera). Membranes were incubated with the serum samples for 2 hours at room temperature and washed with TBST. For blots of TRAMP sera, goat antimouse horseradish peroxidase (HRP)-conjugated secondary antibody (Sigma, St. Louis, MO) was used at 1:5,000 dilution in TBST/5% milk for 1 hour at room temperature. The blots were washed for 1 hour with TBST and HRP developed with enhanced chemiluminescence (ECL). For analysis of human sera, a donkey anti-human biotin conjugated secondary antibody (Jackson ImmunoResearch, West Grove, PA) was used at a 1:50,000 dilution in 1:10 "blocking solution" for 1 hour. After washing with TBST, HRP-conjugated streptavidin was incubated with the blots (1:25,000 dilution in 1:10 blocking solution) for 1 hour, and the blots were subjected to a final wash. Super-Signal ECL (Pierce, Rockford, IL) was used to develop the HRP for the human samples and generic ECL was used for mouse samples (20).

ELISA test for HIP1 autoantibodies. MaxiSorb immunoplates (Nalge Nunc International, Rochester, NY) were coated with 5 μ g/mL of the 3'HIP1 antigen by incubating 50 μ L per well overnight at 4°C . The plates were washed twice with TBST. Plates were blocked with 200 μ L of 5% milk in TBST overnight at 4°C , washed twice with TBST, and stored at 4°C for a maximum of 2 weeks. Serum samples (50 μ L per well) diluted 1:100 in blocking solution were assayed in duplicate and incubated with the antigen-coated plates at room temperature for 1 hour. The plates were washed five times with TBST and incubated with 1:10,000 goat anti-human IgG biotin-conjugated (Pierce) secondary antibody for 30 minutes. The plates were again washed five times with TBST and incubated with avidin-biotin complex reagent (Pierce) for 30 minutes and washed; 100 μ L of the 1-Step Ultra TMB (Pierce) were incubated on the plates for 30 minutes for color development and quenched with 100 μ L of H_2SO_4 . Absorbance was measured at 450 to 550 nm using a VERSAmax microplate reader (Molecular Devices, Sunnyvale, CA).

Statistical analysis. All statistical analyses were done with Excel, Medcalc, or SPSS. To test for the difference in tumor incidence and histologic appearances the MedCalc program was used to perform correlative and χ^2 tests. To test for significant differences in HIP1 immune response between prostate cancer patients and control subjects, Pearson's χ^2 test as well as Student's two-sided *t* test were done using SPSS. ROC curve analysis was achieved using the MedCalc program.

Results

Diminished prostate tumor development in transgenic adenocarcinoma of the mouse prostate/HIP1^{null/null} mice. To examine the *in vivo* necessity of HIP1 overexpression in prostate tumors, TRAMP mice (14) and *Hip1*^{null/null} mice (15) were crossed to generate TRAMP mice deficient of HIP1 (TRAMP/*Hip1*^{null/null} mice) as well as control littermates (TRAMP/*Hip1*^{+/+} mice). This experiment was based on the previous observation that murine HIP1 is overexpressed in 50% of prostate tumors that develop in TRAMP mice (12) and that the loss of function mutation of *Hip1* does not alter the development or maintenance of normal prostate tissue nor does it affect hormone levels in mice including testosterone (15, 17). In an initial study of these mice, we noted that TRAMP mice deficient for HIP1 did not develop as many palpable tumors as their wild-type HIP1 expressing littermates (data not shown). To quantitate this observation, we initiated a second experiment where TRAMP littermates without HIP1 expression (TRAMP/*Hip1*^{null/null}) and their controls (TRAMP/*Hip1*^{+/+}) were sacrificed at 6.5 months of age. We chose to analyze mice at this age, as by 6 months of age, all TRAMP mice develop prostate tumors (18). As seen in Fig. 1A, the absence of HIP1 expression resulted in fewer grossly observed prostate tumors than littermate *Hip1* wild-type controls (2 of 8 TRAMP/*Hip1*^{null/null} [25%] versus 13 of 16 TRAMP/*Hip1*^{+/+} [81%], respectively; *P* < 0.01).

The diminished tumor frequency observed in the *Hip1*^{null/null} mice could be due to a reduced rate of tumor initiation. Alternatively, HIP1 may be required for tumor growth or progression to invasive carcinoma. To begin to distinguish between these possibilities, the histologic characteristics of the prostates and their tumors from these mice was scored using a previously described grading system of prostatic lesions (18). Briefly, serial tissue sections were characterized for their most advanced lesions. For example, "hyperplasia" was scored when the epithelial cells of the acini were crowded and formed foci in cribriform or papillary patterns but still followed the outline of the acinus. "Adenoma" was scored when in some parts of the tissue the epithelial cells completely filled the lumen or distinct epithelial masses were found in the lumen of the acinus. "Invasive carcinoma" was scored when there was local invasion into and beyond the capsule of the acinus or there were distant metastases. The TRAMP mice with "adenomas" or "invasive carcinomas" also contained multiple foci of hyperplasia.

Using this scoring system, we found that development of invasive cancers was diminished in TRAMP/*Hip1*^{null/null} mice. At 6.5 months of age, most of the TRAMP mice with normal *Hip1* had adenomas or invasive cancers (8 of 8 observed TRAMP/

Hip1^{+/+} [100%] versus 1 of 6 [17%] TRAMP/*Hip1*^{null/null}; Fig. 1B). In contrast, most of the TRAMP/*Hip1*^{null/null} mice had only hyperplastic lesions (five of six, 84%). The differences in tumor incidence either by gross observation or by histology between control and TRAMP/*Hip1*^{null/null} mice was significant ($P < 0.01$ and $P < 0.025$, Pearson's χ^2 , respectively). These data suggest that there is a delay in the ability of prostatic lesions from *Hip1*^{null/null} mice to progress from hyperplasia to adenomas and invasive carcinomas. Previously, we reported that 50% of TRAMP prostate tumors overexpressed HIP1 by Western blot analysis of tumors (12). In contrast, we find here that at least 75% of the TRAMP prostates required HIP1 expression for invasive tumor formation (Fig. 1A, first column). This suggests that the sensitivity to detect HIP1 overexpression by Western blot analysis of prostate tumors may be limited.

Autoantibodies to HIP1 in transgenic adenocarcinoma of the mouse prostate mice. Because HIP1 was overexpressed in prostate tumors of both humans and mice (12), we attempted to measure HIP1 levels in mouse serum by Western blot analysis using anti-HIP1 polyclonal (UM323) and monoclonal (1B11) antibodies. Our goal was to determine if HIP1 antigen quantitation could be used as a novel serum biomarker of prostate cancer. As one might expect for a cytoplasmic protein, we were not able to detect the HIP1 antigen in sera (data not shown). Because of this limited sensitivity, we decided to test the hypothesis that a humoral immune response to overexpressed HIP1 marks prostate cancer presence. If such a response was detected, we hypothesized that it could be used as a potential blood test for prostate cancer detection and prognosis.

To begin to test this, recombinant HIP1 (19) was purified (Fig. 2A, left) and immunoblot with specific HIP1 monoclonal antibodies, 4B10 and 1B11, confirmed its identity (Fig. 2A, right). The lower of the two bands on the Western blot was variably seen in different preparations of the purified antigen and was likely the result of degradation during antigen preparation. In an initial pilot Western blot study of mouse sera and 3' HIP1 antigen, we found that there was immune reactivity to the HIP1 antigen in sera from prostate tumor-bearing TRAMP/*Hip1*^{+/+} mice but not control (T antigen negative) or TRAMP/*Hip1*^{null/null} mice (data not shown). Serial serum samples from TRAMP mice and control mice were loaded in a miniblot apparatus (8) to determine the developmental time course and maintenance of autoantibodies to HIP1 in TRAMP mice (Fig. 2B). Remarkably, we found that there was an antibody response to HIP1 that varied in its time of onset (Fig. 2B) but was detected as early as 4 months of age in the TRAMP mice, all of which were expected to have developed prostatic lesions by 6.5 months of age. Twelve of the 22 (55%) TRAMP mice developed sustained immunity. In contrast, none of the 14 (0%) control (T antigen negative) littermates showed sustained presence of autoantibodies to HIP1.

Serum antibodies to HIP1 in human prostate cancer patients. In light of the presence of autoantibodies to HIP1 in prostate cancer-bearing TRAMP mice, we tested if there was an immune response to HIP1 in sera from human prostate cancer patients. Because one gel was only able to assay 25 distinct sera at a time and we had sera from 308 men available for testing, we used the same positive and negative HIP1 reactive sera on each blot as a reference point. This allowed us to quantitate and normalize signals between different blots. Results of one such screen using sera from prostate cancer patients and controls ($n = 23$ for each) are shown in Fig. 3A. Ultimately, the sera from

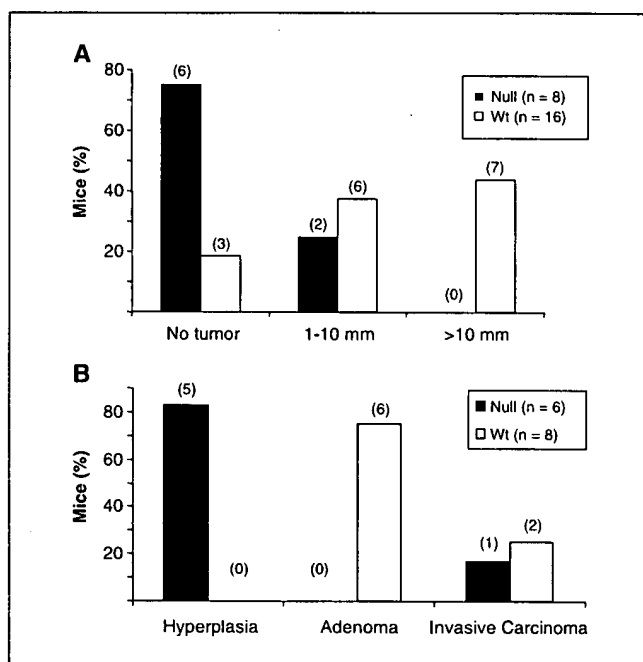


Figure 1. HIP1 deficiency impairs tumorigenesis in the TRAMP model of prostate cancer. **A**, grossly evident tumors were scored during necropsy of TRAMP/*Hip1*^{+/+} ($n = 16$) and TRAMP/*Hip1*^{null/null} ($n = 8$) littermate mice. Observations were recorded as either no obvious tumor, gross tumor of ~1 to 10 mm in diameter or large tumor measuring >10 mm. Most TRAMP/*Hip1*^{null/null} mice had grossly normal prostates (6 of 8) compared to the TRAMP/*Hip1*^{+/+} mice (3 of 16, 75% versus 18.8%, respectively). There were no tumors >10 mm in the absence of HIP1 compared with 7 of 16 in the presence of HIP1. Numbers of mice in each observation are bracketed above the columns. **B**, histologic analysis of prostate tissue from a second cohort of TRAMP mice at 6.5 months of age. Six prostate samples were derived from *Hip1* null prostates and eight prostate samples were derived from *Hip1* wild-type littermates. Serial sections of the prostates were prepared for H&E staining. These slides were scored for the presence of hyperplasia, adenoma, or invasive carcinoma within the prostate (18). Eighty-three percent (five of six) of the *Hip1*^{null/null} mice had only hyperplasia in the prostate tissue. All of the TRAMP/*Hip1*^{+/+} mice were found to have multiple foci of either adenoma (75%) or invasive carcinoma (25%), as expected.

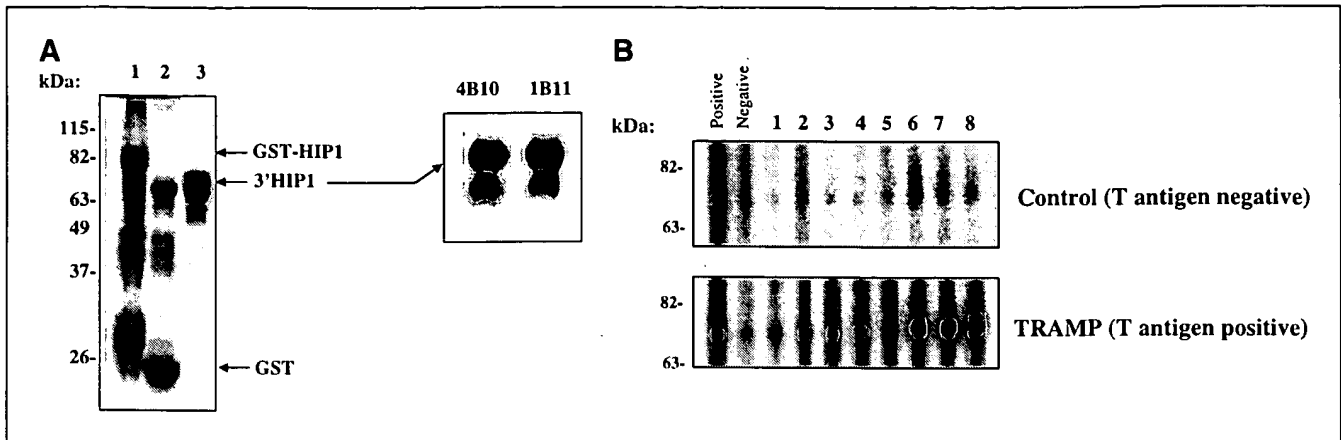


Figure 2. Humoral immune response to HIP1 in TRAMP mice. **A**, purification of recombinant 3'HIP1 protein was achieved in three steps as described in the methods. Lane 1, contains 40 µg of protein from an IPTG-induced bacterial extract bound to and eluted with glutathione from glutathione Sepharose. Lane 2, partially purified thrombin-treated extract. Released GST (bottom arrow) and the HIP1 portion of the recombinant protein (top arrow) were visualized with Coomassie blue stain. Lane 3, 5 µg of the final "purified" recombinant 3'HIP1 protein that was used for assays of a humoral response. This purified recombinant HIP1 was recognized by two different previously described (12) anti-HIP1 monoclonal antibodies (HIP1/4B10 and HIP1/1B11) as shown in the Western blot of 200 ng of antigen (right). **B**, antibodies to HIP1 in TRAMP mice. A group of 22 TRAMP and 14 T antigen negative control mice between the ages of 2 to 4 months, had blood samples drawn every 2 weeks and sera prepared to test for when and if a humoral response to HIP1 might develop. This representative blot shows a control, T antigen-negative mouse (top), and a TRAMP mouse (bottom). Positive and Negative lanes, reference positive (TRAMP/Hip1^{+/+} mouse sera found to be positive in the original screen) and negative (Hip1^{-/-} mouse sera) controls allowing for comparisons of HIP1 reactivity between immunoblots, respectively. Over 16 weeks beginning at age 2.5 months (lanes 1-8) serial serum analysis demonstrated that by 3 months of age a sustained immune response to HIP1 in the TRAMP mice occurred and increased significantly by 5 months of age. It should be noted that sera from T antigen-negative control mice would at times test positive but did not display sustained positive tests.

97 prostate cancer and 211 age-matched male control sera were screened by Western blot. The blots were analyzed by measuring the grayscale values of the reactive bands (Fig. 3A, arrows) and quantitated as a percent of the reference positive control (Fig. 3B). A positive score was assigned to bands with a value of $\geq 50\%$ of the positive control, whereas those bands $< 50\%$ of the positive control received a negative score. This cutoff was chosen because it yielded the highest values for specificity and sensitivity, as analyzed from ROC curves created from a randomly chosen subset of the prostate cancer and control subjects. All serum samples were validated for autoantibodies to HIP1 by this high-throughput immunoblot analysis. HIP1 antibodies were significantly more frequent in serum from prostate cancer patients compared with age-matched controls ($P < 0.001$ χ^2 , likelihood ratio). Forty-five of 97 (46%) prostate cancer patient sera received a positive score compared with 58 of 211 (27%) of the age-matched control sera (Fig. 3C).

For confirmation of our Western blot results and the development of an additional clinical assay, an ELISA to monitor HIP1 immune response was developed. ELISA plates were coated with purified recombinant 3'HIP1, and sera from patients with prostate cancer or age-matched controls were assayed. The measured absorbance was converted to values relative to negative reference controls and duplicate samples in each of two experiments ($n = 4$ replicates) were averaged. Figure 4A shows the average relative absorbencies for all of the prostate cancer patient sera and 81 of the control sera. A relative absorbance that was greater than the negative control (ELISA value, > 1) was considered a positive score. The cutoff for this test was, like the high-throughput Western blot test, determined by using ROC curves on a subset of the patient sera and determining where the ELISA values yielded the highest specificity and sensitivity. All available serum samples were then tested for HIP1 antibodies by high-throughput ELISA. There were

significantly more prostate cancer sera with positive scores (46% of sera from prostate cancer patients versus 27% of sera from age-matched controls; Fig. 4B). The ELISA test alone results in similar values for specificity and sensitivity as the Western blot analysis (Table 2). If both tests are required to be reactive for a positive test, only 24% of the prostate cancers are positive versus 12% of the controls. Although there is diminished sensitivity using the increased stringency (both tests necessarily reactive), it does raise the specificity to 88%. The observed decreased sensitivity with the combination of Western blot and ELISA tests is expected because the chance that both tests, which have distinct antigen presentations on either nitrocellulose membranes or plastic plates, would have accessible antigenic epitopes simultaneously in each patient is less likely than if only one were necessary. Hence, if only one of the two HIP1 reactivity tests is required for positivity, 69% of the prostate cancers are positive versus 44% of the controls (Table 2). It should be noted at this point that the control group did not undergo prostate biopsies or have close follow-up. Because of this limitation, the possibility of missed prostate cancer in the control group must be considered when evaluating this initial data. In addition, some of the "background" could be contributed by other occult malignancies such as melanoma, colon, or lung cancers.

Previously, we have found that using immunohistochemical analysis of HIP1 antigen in tissue sections, overexpression of HIP1 in prostate cancers predicted a poor outcome (12). It follows that the autoantibodies to HIP1 in prostate cancer patients might also contain prognostic information. In the current group of 97 prostate cancer patients, there were no statistically significant associations between HIP1 immune responses and linked clinical variables including initial PSA level, PSA recurrence, Gleason grade, tumor size, or stage.

In addition to assessing the relationship between linked clinical data and HIP1 autoantibody formation, we compared the HIP1 test

to other serum tests such as the PSA and AMACR tests. In the initial study of the AMACR humoral response, a specificity of 71.8% and sensitivity of 61.6% were found (8). The samples used for this current study of HIP1 humoral response were also tested for their humoral immune response to AMACR and similar values for AMACR specificity and sensitivity were found as previously reported (67% and 64%, respectively; Table 2). The ROC curves for HIP1 and AMACR yielded similar values for area under the curve (data not shown).

As well as comparison with the AMACR test, it follows that the HIP1 antibody test could complement the PSA test. However, the comparison of the HIP1 test to the PSA test in the group of patients ($n = 90$) and controls ($n = 117$) for which PSA data was available was problematic. This was due to the availability of only a limited supply of banked serum samples from control patients with PSA values of >4.0 ng/mL. This resulted in an expected but skewed specificity and sensitivity (75% and 77%, respectively) for the PSA test (positive, >4.0 ng/mL). The reported 45% specificity and 50% sensitivity for PSA in a previous group of sera that were tested for AMACR are closer to expected (8). Because of this limited supply, a subgroup of 68 prostate cancer sera and 29 age-matched control sera that had PSA values of >4 ng/mL was analyzed separately for HIP1 autoimmunity (Table 3). There was again a significant difference in the numbers of HIP1-positive samples from prostate cancer patients versus control individuals, as determined by ELISA

or Western blot ($P \leq 0.025$ and $P \leq 0.01$, respectively). The most significant difference was seen when a positive score by either ELISA or Western blot was required, giving a specificity of 64% and a sensitivity of 88% ($P \leq 0.001$) in a group that would all be considered positive by the PSA test. In addition, a combination of AMACR and HIP1 tests increased specificity *dramatically* (97%) suggesting that the combination of these two tests could lead to better predictions of cancer if added to the PSA test. Although further analysis of additional patient and control populations with prospective follow-up, serial sampling (as shown for the TRAMP mice in Fig. 2B) and from multiple different institutions is essential, these results suggest that the combination of the HIP1 test with PSA and AMACR tests results has the potential to yield a highly specific diagnostic test for prostate cancer.

Discussion

Prostate cancer morbidity and mortality are due to its progression within the prostate as well as its metastatic spread beyond the prostate. Because of this, an understanding of the mechanism by which localized hyperplastic lesions progress to invasive and metastatic carcinomas is very important. In addition, obtaining blood tests that can provide for the earliest detection of prostate cancer will have important prognostic and therapeutic implications.

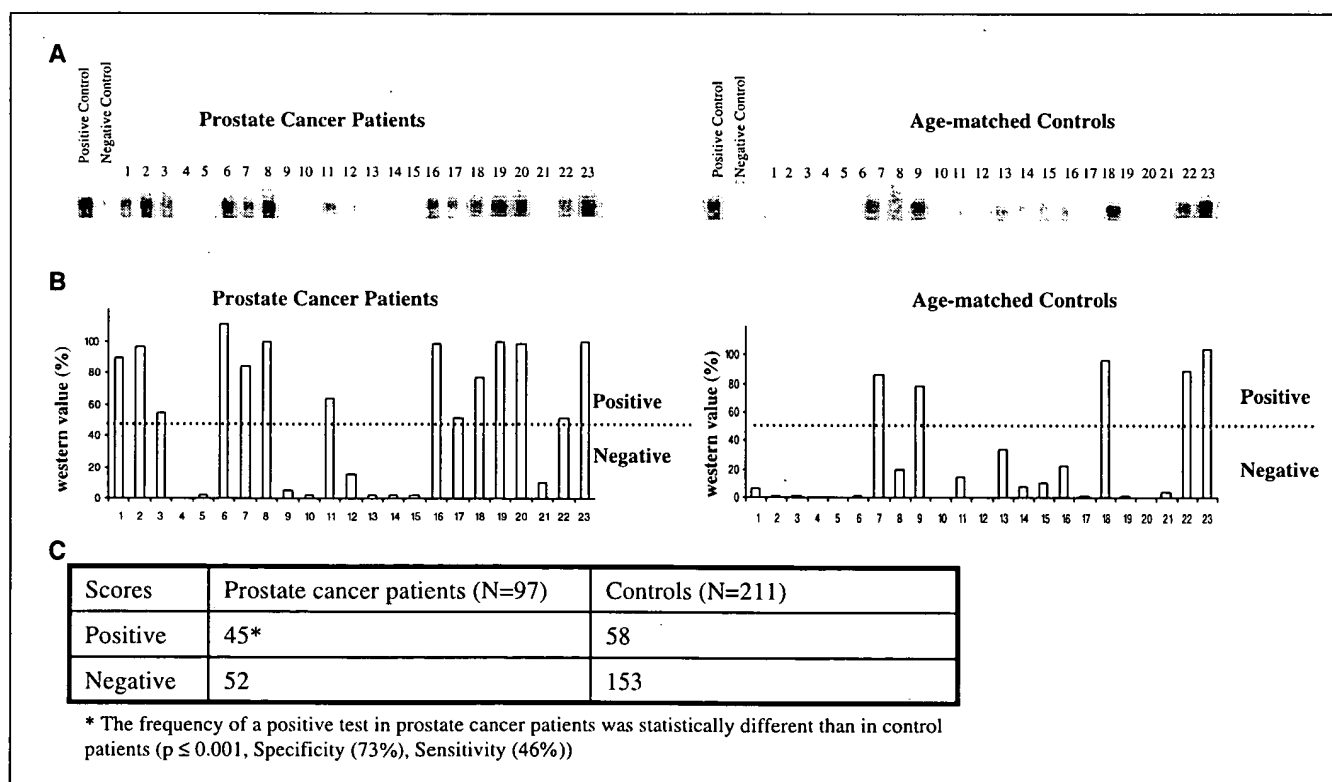


Figure 3. Prostate cancer patients have a specific humoral response to HIP1 overexpression. **A**, representative immunoblot of 46 sera assayed for reactivity to recombinant HIP1. Twenty-three of the 97 biopsy-proven prostate cancer patients and 23 of the 211 control individuals. Equal aliquots of all of the 308 serum samples were analyzed by immunoblot in at least two independent experiments and contained reference positive and negative controls (Positive and Negative lanes, respectively). **B**, bands were scanned from the developed blots and converted to grayscale values using Adobe Photoshop. Normalized grayscale values were converted to percentage of the positive control (Positive lane). Samples with band intensity of $\geq 50\%$ of the positive control were given a positive score (above the dotted line). A negative score was given to samples $<50\%$ of positive control (below the dotted line). **C**, distribution of the values between prostate cancer and the control individuals was significantly different ($P < 0.001$, Pearson's χ^2 test). Specificity of the test was 73% and calculated as those control samples with a negative test (153/153 + 58) and sensitivity was 46% and calculated as the percent of patient samples with a positive test (45/45 + 52).

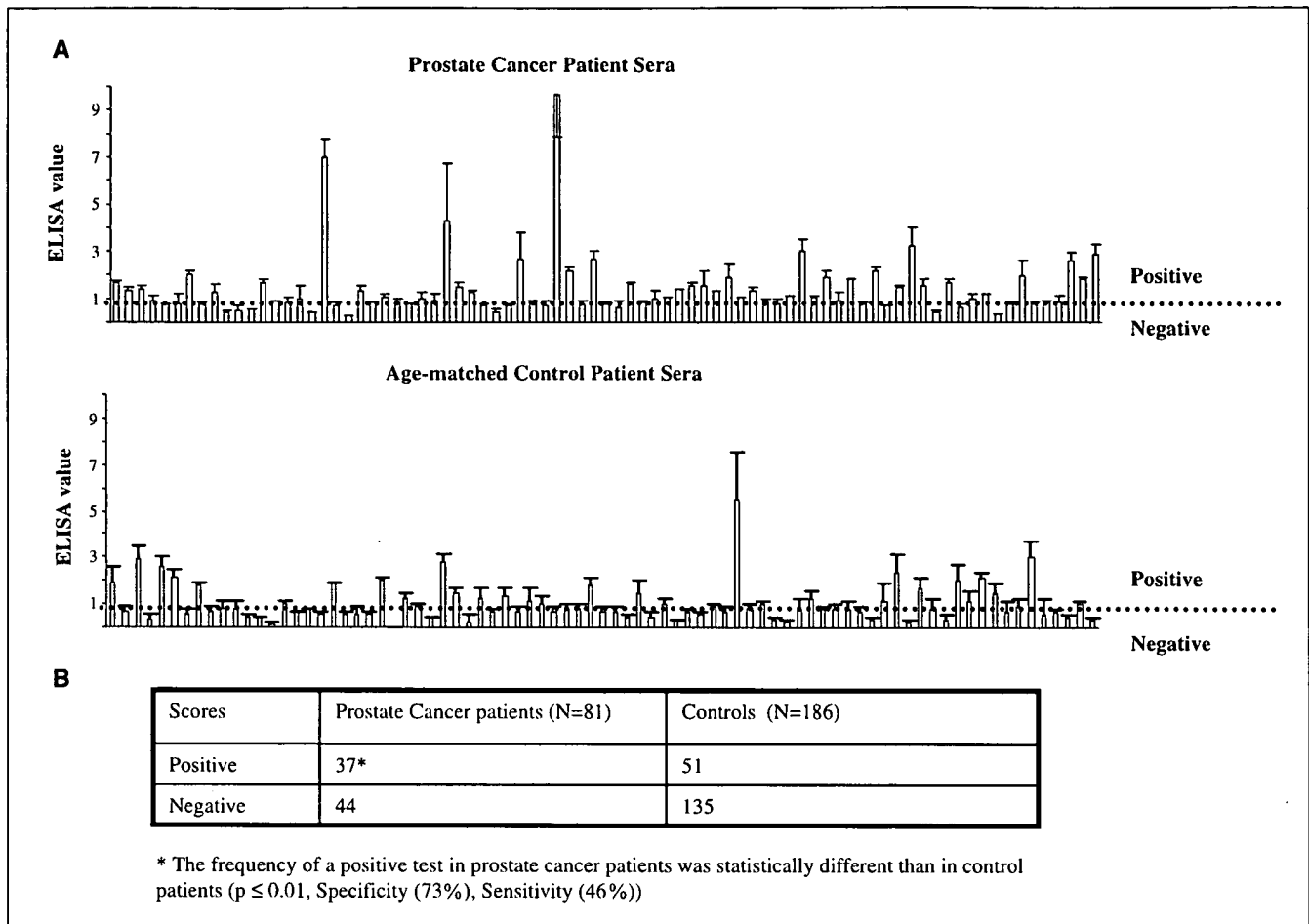


Figure 4. Detection of HIP1 humoral response in human prostate cancer patients by ELISA. **A**, average (four replicates) relative absorbances (ELISA values) and their standard deviations are shown for 81 prostate cancer patient and 186 control sera. A relative absorbance of >1.0 (above the dotted line) was considered positive. **B**, numbers of positive prostate cancer and age-matched control sera. The specificity of this test was 73% and the sensitivity was 46%. The difference between prostate cancer patients and controls was significant ($P < 0.01$, Pearson's χ^2).

Here we report *in vivo* genetic evidence for the necessity of the clathrin-binding protein, HIP1, in the prostatic hyperplasia-to-carcinoma transition. These experiments were initiated based on the fact that HIP1 expression is frequently elevated in human prostate cancer, and this overexpression predicts the progression of the disease in humans. In addition, because TRAMP mice have HIP1 up-regulated in their tumors (12), it was considered a relevant tumor model. We show that although all *Hip1*^{null/null} mice developed prostatic hyperplastic lesions in response to expression of T antigen, the development of bona fide tumors was significantly diminished compared with TRAMP mice with normal levels of HIP1.

Although the absence of HIP1 leads to testicular degeneration, it should be noted that the prostate glands from *Hip1* knockout mice are normal histologically and serum testosterone levels are within normal limits (15, 17). This makes it unlikely that the effect of HIP1 deficiency on tumor development in this model is merely secondary to differences in the levels of testosterone or abnormalities in adult prostate epithelial cell maintenance. It should also be noted that the use of SV40 T antigen to induce prostate cancer is, in many ways, artificial in that T antigen does not seem to have a role in human prostate cancer. However, because HIP1 is overexpressed in TRAMP tumors, as it is in

human tumors, and because T antigen does inhibit the human tumor suppressor gene products p53 and Rb, this model has significant validity for the purposes of initial studies of HIP1's *in vivo* role in cancer biology.

It will be important to better understand the mechanism of how HIP1 could participate in the development of prostate cancer in humans. Previous work has shown that the HIP1 family of proteins is involved in the modulation of a variety of receptors such as the glutamate receptor (21), the epidermal growth factor receptor (EGFR), platelet-derived growth factor β receptor (PDGF β R; ref. 22), and transferrin receptor (23). This modulation of receptors leads to an increased survival and transformation of cells when HIP1 is overexpressed (12, 13). Although a direct regulatory effect of HIP1 on clathrin trafficking in prostate cancer remains to be shown, HIP1 could modulate signals from the EGFR and PDGF β R in prostate cancer as these receptors are clearly regulated by the clathrin trafficking network and are altered in prostate cancer. Determination if HIP1 can modulate other types of receptors that are not regulated by clathrin-mediated endocytosis but are involved in prostate cancer, such as the steroid hormone receptors (e.g., androgen receptor), will be important future experiments.

In addition to testing for HIP1 necessity in prostatic carcinogenesis, the previous observation of HIP1 overexpression in tumors

of TRAMP mice (12) prompted us to test if HIP1 could be detected in the serum of these mice. As expected for a cytoplasmic protein, we found that the circulating HIP1 antigen levels are low and therefore difficult to detect. However, we did find that TRAMP mice developed early and sustained levels of antibodies against HIP1 when measuring longitudinal samples. Interestingly, the T antigen-negative control mice also had samples of sera that tested positive randomly. However, sustained presence of anti-HIP1 antibodies were never observed in the control mice.

This led us to test if a humoral response to HIP1 could occur in humans with prostate cancer. The goal would be to find a novel blood test to substitute for or to complement the PSA test. Indeed, the test we describe herein for autoantibodies to HIP1 in prostate cancer has a relatively high specificity and improves the specificity of the PSA and AMACR tests, making it an attractive serum marker. Because we were able to show a sustained humoral response in TRAMP mice, we predict that future studies that are designed for prospective serial testing of humans for HIP1 antibodies will show an increase in the anti-HIP1 test's sensitivity and specificity. Because prostate cancer is such a common cancer, markers with a greater specificity rather than sensitivity are needed to reduce unnecessary prostate biopsies or other invasive tests. For example, misdiagnosis with the PSA test may account for >30% of positive tests in a screened male population over the age of 55 (24), making reliance on the PSA test alone problematic. Finally, it is unlikely that any single marker for prostate cancer will have the desired high specificity and sensitivity, making it important to develop a collection of markers, which in combination could lead to accurate prostate cancer detection and prognosis.

Table 2. Comparison of diagnostic tests and their combinations for all prostate cancer and control samples

Test	Specificity (%)	Sensitivity (%)
HIP1 ELISA positive*	73	46
HIP1 western positive†	73	46
HIP1 ELISA + HIP1 Western positive‡	88	24
HIP1 ELISA or HIP1 Western positive‡	56	69
AMACR positive†	67	64
AMACR positive + HIP1 ELISA or HIP1 Western positive‡	86	50
PSA positive (≥4 ng/mL)†	75	77
PSA positive + HIP1 ELISA or HIP1 Western positive‡	91	66

NOTE: There were a total of 97 prostate cancer and 211 control sera. Not all of these 308 sera, except for the HIP1 Western, were assayed for every test listed. HIP1 ELISA values were available from 81 of the prostate cancer patients and 186 controls. AMACR Western values were available for 77 prostate cancer patients and 126 controls. PSA values were available for 90 prostate cancer patients and 117 controls. The increased frequency of a positive test in prostate cancer patients compared with controls was statistically different in all cases.

* $P \leq 0.01$.

† $P \leq 0.001$.

‡ $P \leq 0.025$.

Table 3. Comparison of diagnostic tests and their combinations for all prostate cancer and control samples with PSA values of ≥4 ng/mL

Test	Specificity (%)	Sensitivity (%)
HIP1 ELISA positive*	76	49
HIP1 Western positive†	82	54
HIP1 ELISA + HIP1 Western positive*	93	28
HIP1 ELISA or HIP1 Western positive‡	64	88
AMACR positive‡	83	64
AMACR positive + HIP1 ELISA or HIP1 Western positive‡	97	55

NOTE: There were 68 prostate cancer and 29 control sera that met the criterion of PSA of ≥4 ng/mL. Nine of the 68 prostate cancer patient sera were not available to test for HIP1 ELISA and AMACR Western. The increased frequency of a positive test in prostate cancer patients compared to controls was statistically different in all cases.

* $P \leq 0.025$.

† $P \leq 0.01$.

‡ $P \leq 0.001$.

The increase in frequency of antibodies to HIP1 in prostate cancer compared with age-matched controls, together with the fact that we had previously found that HIP1 is overexpressed in many different epithelial cancers (12), will prompt us to investigate the potential for a specific humoral response in other cancers. This could also be a source of error in reducing the specificity of the HIP1 blood test for prostate cancer in our current control group, as the men could have had other occult or nonoccult malignancies. In fact, a specific humoral response to the HIP1-related protein, the only known mammalian relative of HIP1, has been reported to occur in colon cancer (25).

In conclusion, we have explored the role of HIP1 in *in vivo* tumorigenesis using the prostate cancer prone TRAMP mice and *Hip1* knockout mice. Our data indicate that HIP1 may be necessary for tumorigenesis and that both mice and men with prostate cancer have autoantibodies to HIP1 in their serum. These data provide groundwork for further investigation into the functional involvement of HIP1 in other cancers and as a specific marker (especially in combination with AMACR) for other cancers. These data also pave the way for further prospective, longitudinal, and multi-institutional studies of how to best use the HIP1 Western blot and ELISA tests for improved care of patients with prostate cancer.

Acknowledgments

Received 1/3/2005; revised 2/11/2005; accepted 2/18/2005.

Grant support: Komen Foundation predoctoral fellowship (S.V. Bradley), La Ligue Nationale contre le Cancer postdoctoral fellowship (G. Bougeard), NIH-R01 CA82363-01A1 (T.S. Ross), NIH-R01 CA098730-02 (T.S. Ross), and NIH-R01 CA82419-01 (M.G. Sanda).

The costs of publication of this article were defrayed in part by the payment of page charges. This article must therefore be hereby marked *advertisement* in accordance with 18 U.S.C. Section 1734 solely to indicate this fact.

We thank Teresa Hyun, Sean Morrison, Anj Dlugosz, Peter Lucas, Grant Rowe, and Mark Day for critically reading this article and Dan Normolle, Jason Harwood, Paul Nolan, June Escara-Wilke, Jenny Loveridge, and Melissa Rogers for their assistance during the course of this study.

References

- Catalona WJ, Smith DS, Ratliff TL, et al. Measurement of prostate-specific antigen in serum as a screening test for prostate cancer. *N Engl J Med* 1991;324:1156-61.
- Etzioni R, Legler JM, Feuer EJ, Merrill RM, Cronin KA, Hankey BF. Cancer surveillance series: interpreting trends in prostate cancer. Part III. Quantifying the link between population prostate-specific antigen testing and recent declines in prostate cancer mortality. *J Natl Cancer Inst* 1999;91:1033-9.
- Maattanen L, Auvinen A, Stenman UH, et al. European randomized study of prostate cancer screening: first-year results of the Finnish trial. *Br J Cancer* 1999;79:1210-4.
- Schroder FH, van der Maas P, Beemsterboer P, et al. Evaluation of the digital rectal examination as a screening test for prostate cancer. Rotterdam section of the European Randomized Study of Screening for Prostate Cancer. *J Natl Cancer Inst* 1998;90:1817-23.
- Thompson IM, Pauler DK, Goodman PJ, et al. Prevalence of prostate cancer among men with a prostate-specific antigen level ≤ 4.0 ng per milliliter. *N Engl J Med* 2004;350:2239-46.
- Punglia RS, D'Amico AV, Catalona WJ, Roehl KA, Kuntz KM. Effect of verification bias on screening for prostate cancer by measurement of prostate-specific antigen. *N Engl J Med* 2003;349:335-42.
- Catalona WJ. Management of cancer of the prostate. *N Engl J Med* 1994;331:996-1004.
- Sreekumar A, Laxman B, Rhodes DR, et al. Humoral immune response to α -methylacyl-CoA racemase and prostate cancer. *J Natl Cancer Inst* 2004;96:834-43.
- McNeel DG, Nguyen LD, Storer BE, Vessella R, Lange PH, Disis ML. Antibody immunity to prostate cancer associated antigens can be detected in the serum of patients with prostate cancer. *J Urol* 2000;164:1825-9.
- Mintz PJ, Kim J, Do KA, et al. Fingerprinting the circulating repertoire of antibodies from cancer patients. *Nat Biotechnol* 2003;21:57-63.
- Nilsson BO, Carlsson L, Larsson A, Ronquist G. Autoantibodies to prostasomes as new markers for prostate cancer. *Ups J Med Sci* 2001;106:43-9.
- Rao DS, Hyun TS, Kumar PD, et al. Huntingtin-interacting protein 1 is overexpressed in prostate and colon cancer and is critical for cellular survival. *J Clin Invest* 2002;110:351-60.
- Rao DS, Bradley SV, Kumar PD, et al. Altered receptor trafficking in Huntingtin interacting protein 1-transformed cells. *Cancer Cell* 2003;3:471-82.
- Greenberg NM, DeMayo F, Finegold MJ, et al. Prostate cancer in a transgenic mouse. *Proc Natl Acad Sci U S A* 1995;92:3439-43.
- Oravec-Wilson KI, Kiel MJ, Li L, et al. Huntingtin Interacting Protein 1 mutations lead to abnormal hematopoiesis, spinal defects and cataracts. *Hum Mol Genet* 2004;13:851-67.
- Shappell SB, Thomas GV, Roberts RL, et al. Prostate pathology of genetically engineered mice: definitions and classification. The consensus report from the Bar Harbor meeting of the Mouse Models of Human Cancer Consortium Prostate Pathology Committee. *Cancer Res* 2004;64:2270-305.
- Rao DS, Chang JC, Kumar PD, et al. Huntingtin interacting protein 1 is a clathrin coat binding protein required for differentiation of late spermatogenic progenitors. *Mol Cell Biol* 2001;21:7796-806.
- Suttie A, Nyska A, Haseman JK, Moser GJ, Hackett TR, Goldsworthy TL. A grading scheme for the assessment of proliferative lesions of the mouse prostate in the TRAMP model. *Toxicol Pathol* 2003;31:31-8.
- Saint-Dic D, Chang SC, Taylor GS, Provot MM, Ross TS. Regulation of the Src homology 2-containing inositol 5-phosphatase SHIP1 in HIP1/PDGF β R-transformed cells. *J Biol Chem* 2001;276:21192-8.
- Kricka LJ. Chemiluminescent and bioluminescent techniques. *Clin Chem* 1991;37:1472-81.
- Metzler M, Li B, Gan L, et al. Disruption of the endocytic protein HIP1 results in neurological deficits and decreased AMPA receptor trafficking. *Embo J* 2003;22:3254-66.
- Hyun TS, Rao DS, Saint-Dic D, et al. HIP1 and HIP1r stabilize receptor tyrosine kinases and bind 3-phosphoinositides via epsin N-terminal homology domains. *J Biol Chem* 2004;279:14294-306.
- Engqvist-Goldstein AE, Drubin DG. Actin assembly and endocytosis: from yeast to mammals. *Annu Rev Cell Dev Biol* 2003;19:287-332.
- Draisma G, Boer R, Otto SJ, et al. Lead times and overdiagnosis due to prostate-specific antigen screening: estimates from the European Randomized Study of Screening for Prostate Cancer. *J Natl Cancer Inst* 2003;95:868-78.
- Scanlan MJ, Welt S, Gordon CM, et al. Cancer-related serological recognition of human colon cancer: identification of potential diagnostic and immunotherapeutic targets. *Cancer Res* 2002;62:4041-7.

**This Page is Inserted by IFW Indexing and Scanning
Operations and is not part of the Official Record**

BEST AVAILABLE IMAGES

Defective images within this document are accurate representations of the original documents submitted by the applicant.

Defects in the images include but are not limited to the items checked:

- ☐ **BLACK BORDERS**
- ☐ **IMAGE CUT OFF AT TOP, BOTTOM OR SIDES**
- ☐ **FADED TEXT OR DRAWING**
- ☐ **BLURRED OR ILLEGIBLE TEXT OR DRAWING**
- ☐ **SKEWED/SLANTED IMAGES**
- ☐ **COLOR OR BLACK AND WHITE PHOTOGRAPHS**
- ☐ **GRAY SCALE DOCUMENTS**
- ☐ **LINES OR MARKS ON ORIGINAL DOCUMENT**
- ☐ **REFERENCE(S) OR EXHIBIT(S) SUBMITTED ARE POOR QUALITY**
- ☐ **OTHER:** _____

IMAGES ARE BEST AVAILABLE COPY.

As rescanning these documents will not correct the image problems checked, please do not report these problems to the IFW Image Problem Mailbox.